

Supporting Information

Multifunctional Polymer-Capped Mesoporous Silica Nanoparticles for pH-Responsive Targeted Drug Delivery

Stefan Niedermayer^{1#}, Veronika Weiss^{1#}, Annika Herrmann^{2#}, Alexandra Schmidt¹, Stefan Datz¹, Katharina Müller², Ernst Wagner², Thomas Bein^{1*} and Christoph Bräuchle^{1*}

¹Department of Chemistry, Nanosystems Initiative Munich (NIM) and Center for Nano Science (CeNS), University of Munich (LMU), Butenandtstr. 11 (E), 81377 Munich, Germany

²Department of Pharmacy, Pharmaceutical Biotechnology, Nanosystems Initiative Munich (NIM) and Center for Nano Science (CeNS), University of Munich (LMU), Butenandtstr. 5-13, 81377 Munich, Germany

authors contributed equally to this work

*corresponding authors: bein@lmu.de, Christoph.Braeuchle@cup.uni-muenchen.de

S1. Synthesis Scheme

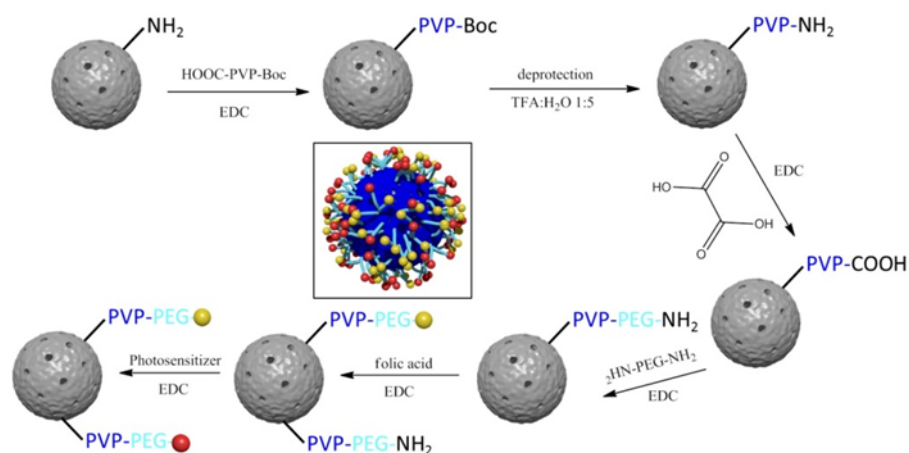


Figure S1: Synthesis scheme of a fully functionalized mesoporous silica nanoparticle (MSN).

S2. Infrared spectroscopy

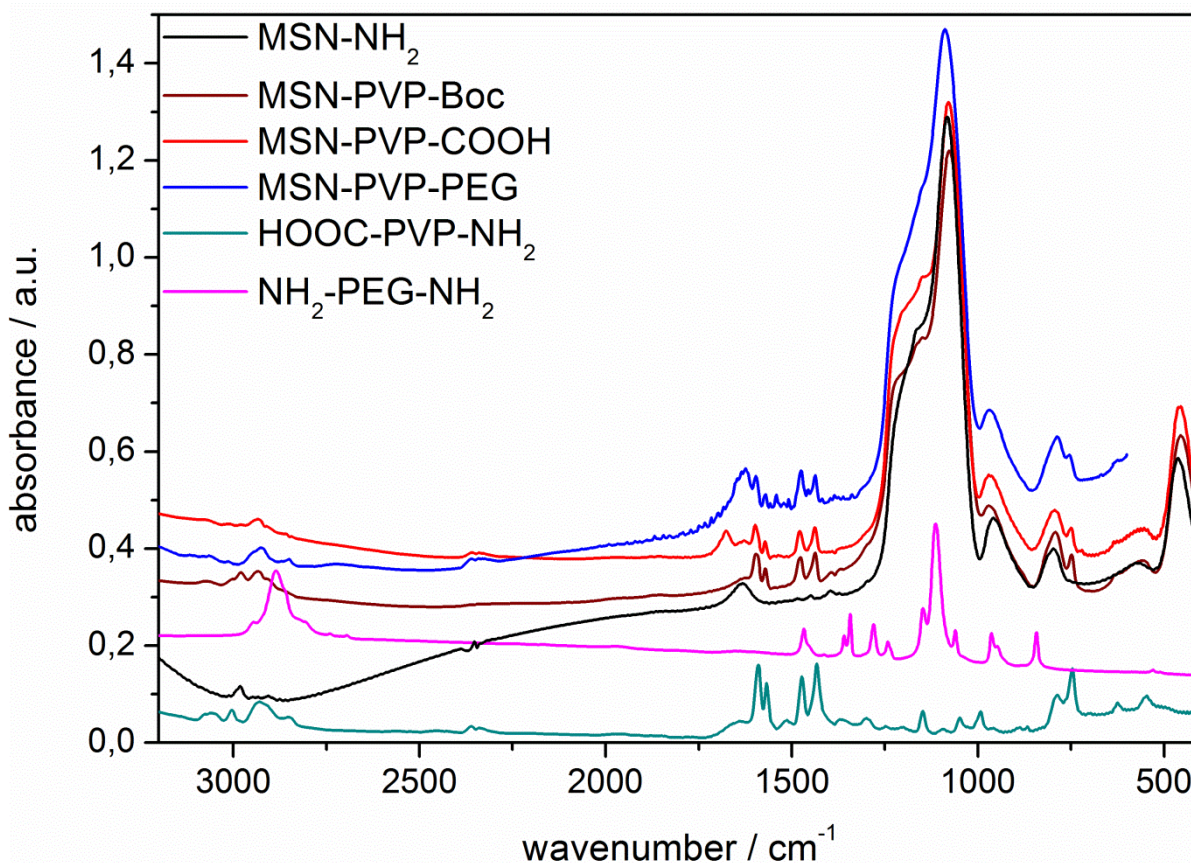


Figure S2. IR spectra of MSN-NH₂ (black), MSN-PVP-Boc (brown), MSN-PVP-COOH (red), MSN-PVP-PEG (blue), HOOC-PVP-NH₂ and NH₂-PEG-NH₂.

Infrared spectroscopy was carried out to prove the functionality of the designed MSN carrier system and to monitor the subsequent reaction steps on the outer shell of the MSNs. The signals between 2850 cm⁻¹ and 2800 cm⁻¹ can be attributed to the CH₂ stretching vibrations arising from the organic functionality (aminopropyl-moieties) and are present in each sample. Furthermore, several peaks at 2900 cm⁻¹ (C-H stretching vibrations) and at 1400 cm⁻¹ (C-H bending vibrations) are visible. The peaks at 1590 cm⁻¹ and 1570 cm⁻¹ correspond to the C=C stretch vibrations of the aromatic pyridine ring and are present in each spectra after the attachment of PVP to the surface of MSN-NH₂. Additionally, peaks at 1474 cm⁻¹ and 1430 cm⁻¹ are present after covalent

attachment of the boc-protected polymer to the shell of the MSNs and can be assigned to the C=N stretch vibrations of the aromatic pyridine ring. In order to successfully enable additional covalent attachment of functionalities (e.g. PEG or targeting ligands), the boc-protection group at the polymer end was subsequently removed (cf. appendix 5.8). After deprotection of MSN-PVP-NH₂-Boc and conversion of the amino group into a carboxy-functionality with oxalic acid, a peak at 1677 cm⁻¹ arises which can be attributed to the asymmetric C=O stretching vibration of MSN-PVP-COOH. This band shifts after PEGylation, implying a successful attachment of PEG.

S3. Raman measurements

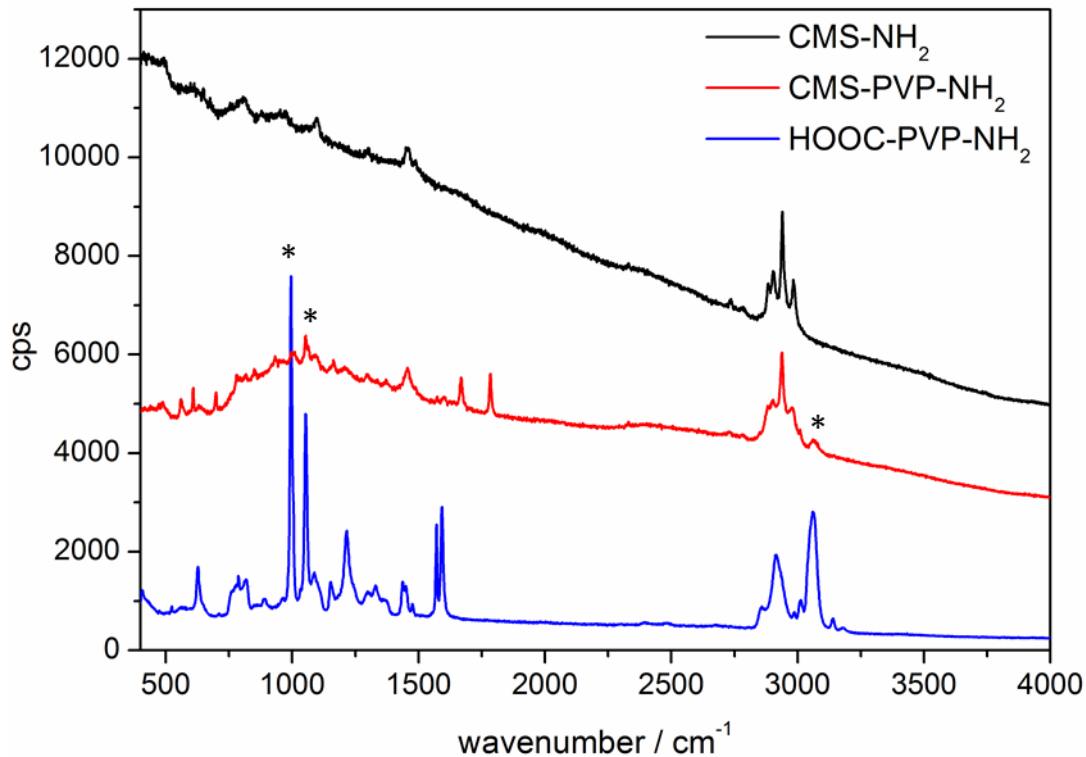


Figure S3. Raman spectra of MSN- NH_2 (black), MSN-PVP- NH_2 (red) and HOOC-PVP- NH_2 (blue).

In addition, Raman spectroscopy was used to monitor the attachment of HOOC-PVP- NH_2 (Figure S4, blue curve) to MSN- NH_2 (Figure S3, black curve) resulting in MSN-PVP- NH_2 (Figure S4, red curve). Bands at 3062 cm^{-1} (*) (C-H stretching vibration of aromatic rings (pyridine)) and 1054 & 995 cm^{-1} (*) (ring stretching vibration of mono-substituted pyridines) are typical for the pyridine groups of poly-2-vinylpyridine. The signals from the polymer appear in the MSN sample after attachment of PVP to MSN and are marked with an asterisk.

S4. Zeta potential measurements

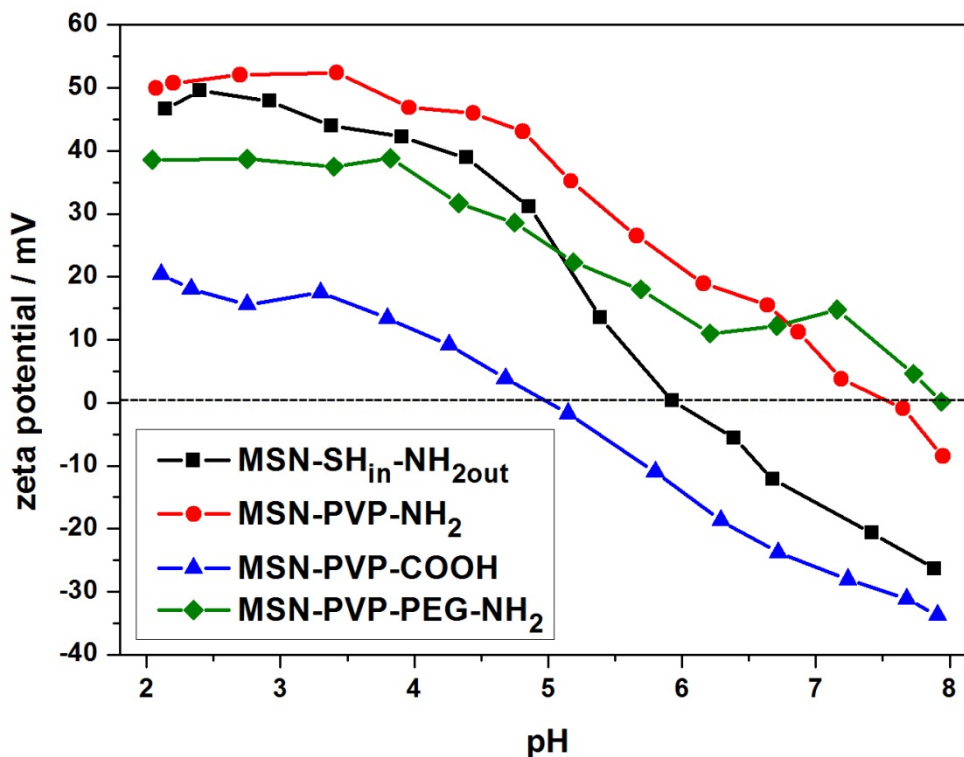


Figure S4. Zeta potential measurements of MSN-NH₂ (black), MSN-PVP-NH₂ (red), MSN-PVP-COOH (blue) and MSN-PVP-PEG-NH₂ (green).

The subsequent attachment of oxalic acid to the sample MSN-PVP-NH₂ was monitored with zeta potential titration measurements. A decrease of zeta potential could be observed due to the low protonation ability of the carboxy-moieties. The successful PEGylation with a bi-functional PEG-linker to the sample MSN-PVP-COOH results in a higher zeta potential values (green curve). In comparison to the carboxy-moieties the terminal amino-groups can be easily protonated at low pH-values. We explain the slightly different zeta potential values between the samples MSN-PVP-NH₂ (red curve) and MSN-PVP-PEG-NH₂ (green curve) with steric hindrances that might be present.

S5. Long-term release experiments

S5.1. Fluorescence spectroscopy

Experimental Setup

Fluorescence experiments were performed to show the time-dependent release of fluorescein from the mesopores of colloidal mesoporous silica spheres. The measurements were recorded on a PTI fluorescence system featuring a PTI 814 photomultiplier detector and an PTI A1010B Xenon arc lamp driven by a PTI LPS-220B lamp power supply. For temperature settings, a Quantum Northwest TC 125 sample holder was used. Fluorescein was excited with 490 nm and emission



Figure S5. Custom made release experiment setup featuring a 200 μL Teflon tube (a) which is closed by a dialysis membrane (b). This setup is put onto a fluorescence cuvette filled with the desired buffer (c).

was detected at 512 nm (excitation slit 1.0 mm, emission slit 1.0 mm, 1 point per 30 min). For the release experiment, a ROTH Visking Typ 8/32 dialysis membrane with a molecular cut-off of 14000 g/mol was used. An image of this custom made Teflon container can be seen in Figure S5.

1 mg MSN were loaded by redispersing them in 500 μL of a 1 mM fluorescein solution that was acidified with 50 μL of a citrate/phosphate buffer of pH 2. After 12 h, the particles were washed by centrifugation and redispersion in SSC buffer pH 7 until no fluorescence was observed in the supernatant. For the release experiment, the particles were redispersed in 200 μL SSC buffer pH 7 and put into a container that was subsequently closed by a dialysis membrane. The closed

container was then put onto a fluorescence cuvette, which was completely filled with SSC buffer pH 7. The released dye is able to pass through the applied membrane while the relatively larger particles are retained. After 16 h, the particles were centrifuged and redispersed in 200 μ L Mc Ilvaine's buffer pH 5, put into the container and closed by the dialysis membrane. The closed container was then put onto the fluorescence cuvette, which was completely filled with Mc Ilvaine's buffer pH 5. The release was measured every 30 min until no further release was observed (Figure S6).

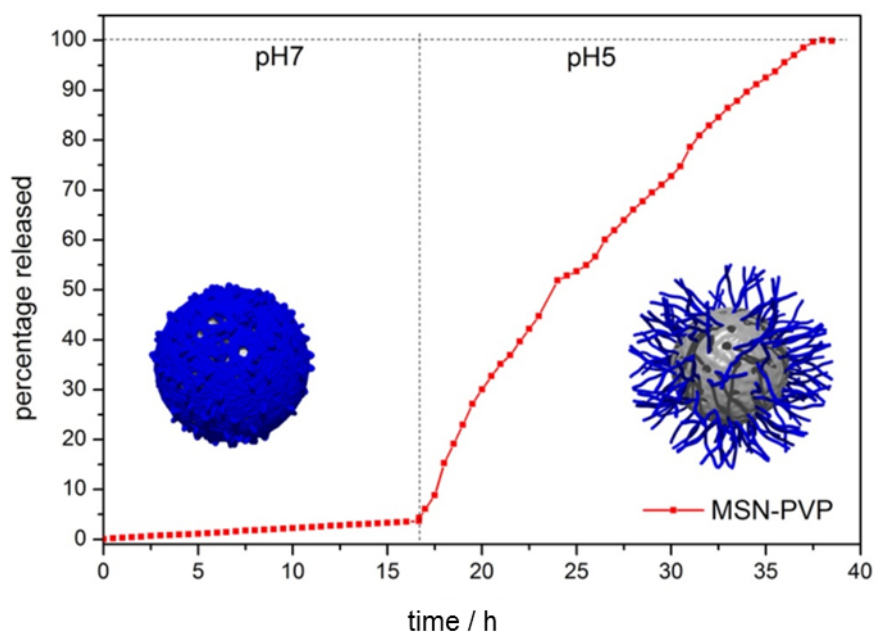


Figure S6. Long term release curve for MSN-PVP-NH₂ loaded with fluorescein (normalized fluorescence intensity).

As the fluorescence of fluorescein is strongly dependent on the pH, calibration curves at pH 7 and pH 5 were recorded (Figure S7) to be able to compare fluorescence signals in the closed and open state.

As the fluorescence of fluorescein is strongly dependent on the pH, calibration curves at pH 7 and pH 5 were recorded (Figure S7) to be able to compare fluorescence signals in the closed and open state.

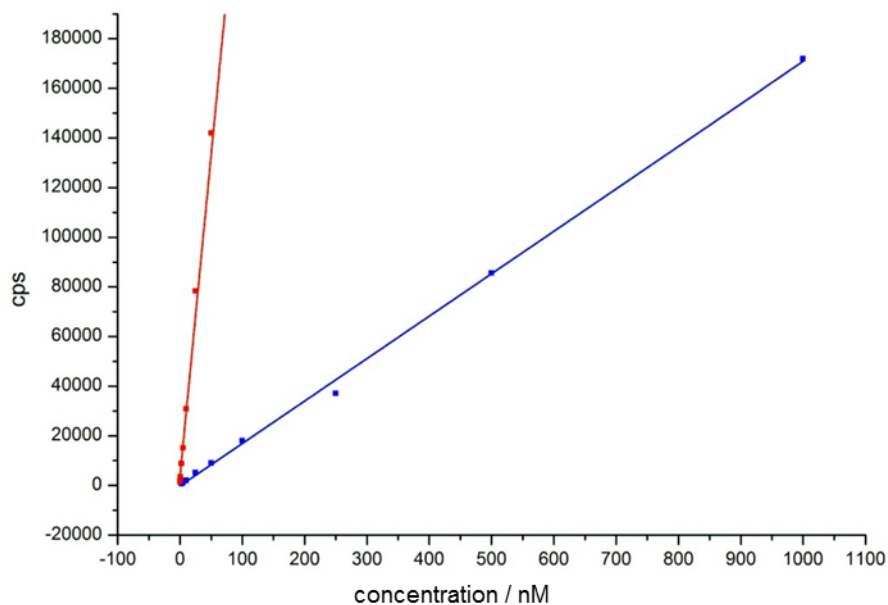


Figure S7. Fluorescein calibration curves at pH 7 (red) and pH 5 (blue) for release measurements in Figure 4 and S6.

S5. UV-Vis spectroscopy

The loading capacity of the particles was quantified with UV-Vis spectroscopy. 1 mg of particles were loaded with 500 μg calcein and washed as described above. The absorption of the supernatants was measured on a Thermo Scientific PeQLab Nanodrop 2000c. Afterwards the particles were stirred for 48 h in 1 mL Mc Ilvaine's buffer pH 5, centrifuged and the absorption of the supernatant was measured again. For determination of the calcein concentration, calibration curves of calcein in Mc Ilvaine's buffer pH 5 and SSC buffer pH 7 at 495 nm were recorded (Figure S8).

The calcein supernatant solution after loading was diluted by the factor of 20. The measured absorbance at 495 nm for the loading capacity of 0.155 leads to an amount of 432 μg by using the calibration curve's linear regression. After several washing steps with SSC buffer to close the

pore system, the supernatants were collected and measured. The measured absorbance of 0.151 leads to an additional amount of 16 μg . Consequently, the total amount of calcein loaded in 1 mg MSN was 0.052 mg.

⇒ Loading capacity: 0.05 mg/mg MSN

The released amount of calcein was then measured as described above. The measured absorbance at 495 nm of 0.147 leads to an amount of 21 μg by using the calibration curve's linear regression.

The total amount of calcein released from 1 mg MSN was 0.021 mg.

⇒ Release capacity: 0.02 mg/mg MSN

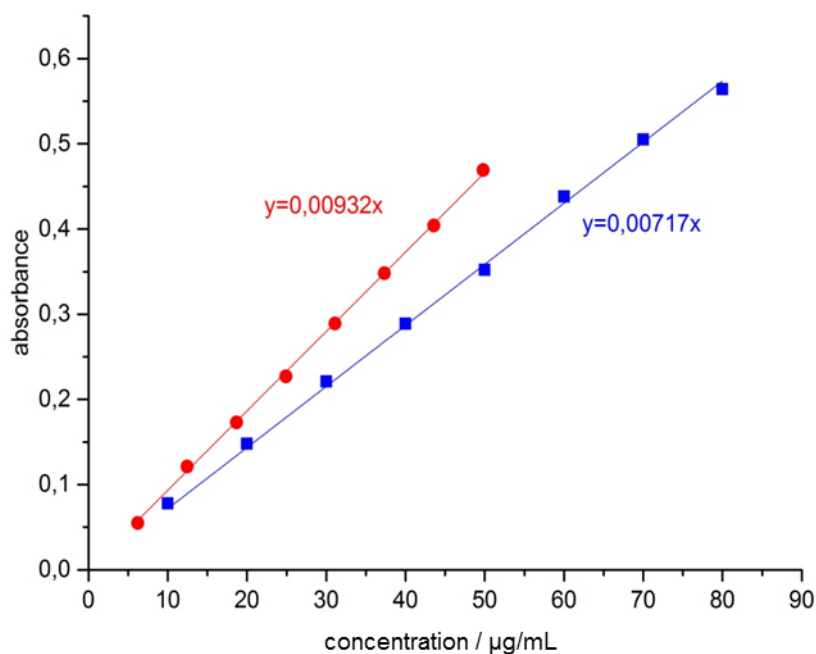


Figure S8. Calcein calibration curves for determination of loading and release capacity at pH 7 (red) and pH 5 (blue).

S7. Further cell experiments

S7.1. Release behavior of the membrane impermeable cargo calcein.

MSN-PVP-PEG particles loaded with calcein were incubated on HeLa cells for 20 h. The

incubation time is long enough to allow the endosomal acidification.^[1] However, as seen in Figure S9, the fluorescence colocalization of the membrane-impermeable cargo calcein and the covalently bound dye Atto 633 remained. Calcein is a membrane impermeable cargo and therefore is not able to exit intact endosomal compartments without external trigger, but it should be released inside the endosomal compartment. In the absence of photosensitizer no release could be detected.

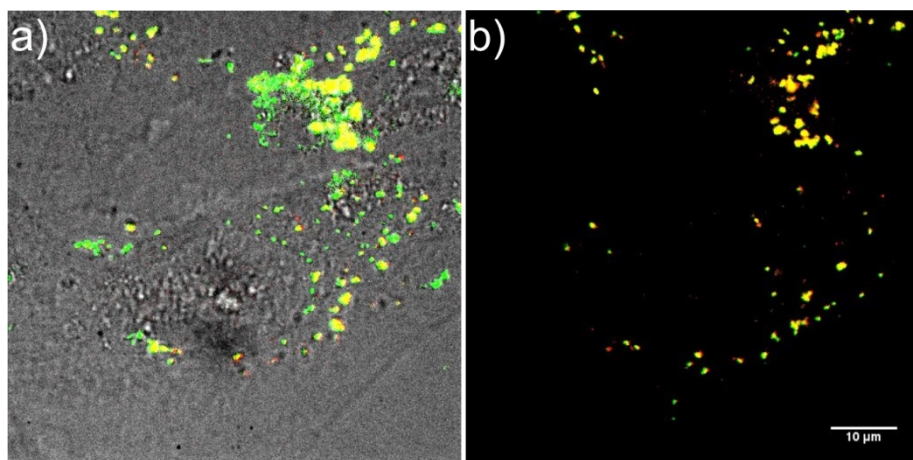


Figure S9. Fluorescence microscopy of MSN(Atto633)-PVP-PEG (25 $\mu\text{g}/\text{mL}$) nanoparticles loaded with calcein inside HeLa cells after 20 h incubation. a) merge of brightfield image and fluorescence image. b) fluorescence image of calcein (green) and Atto633 (red) are co-localized (yellow), no spreading of calcein can be observed, thus no endosomal escape has occurred. The scale bar represents 10 μm .

With additional attachment of the photosensitizer ALPcS_{2a} the release and therefore the increase of the cargo fluorescence inside the cell could be detected.

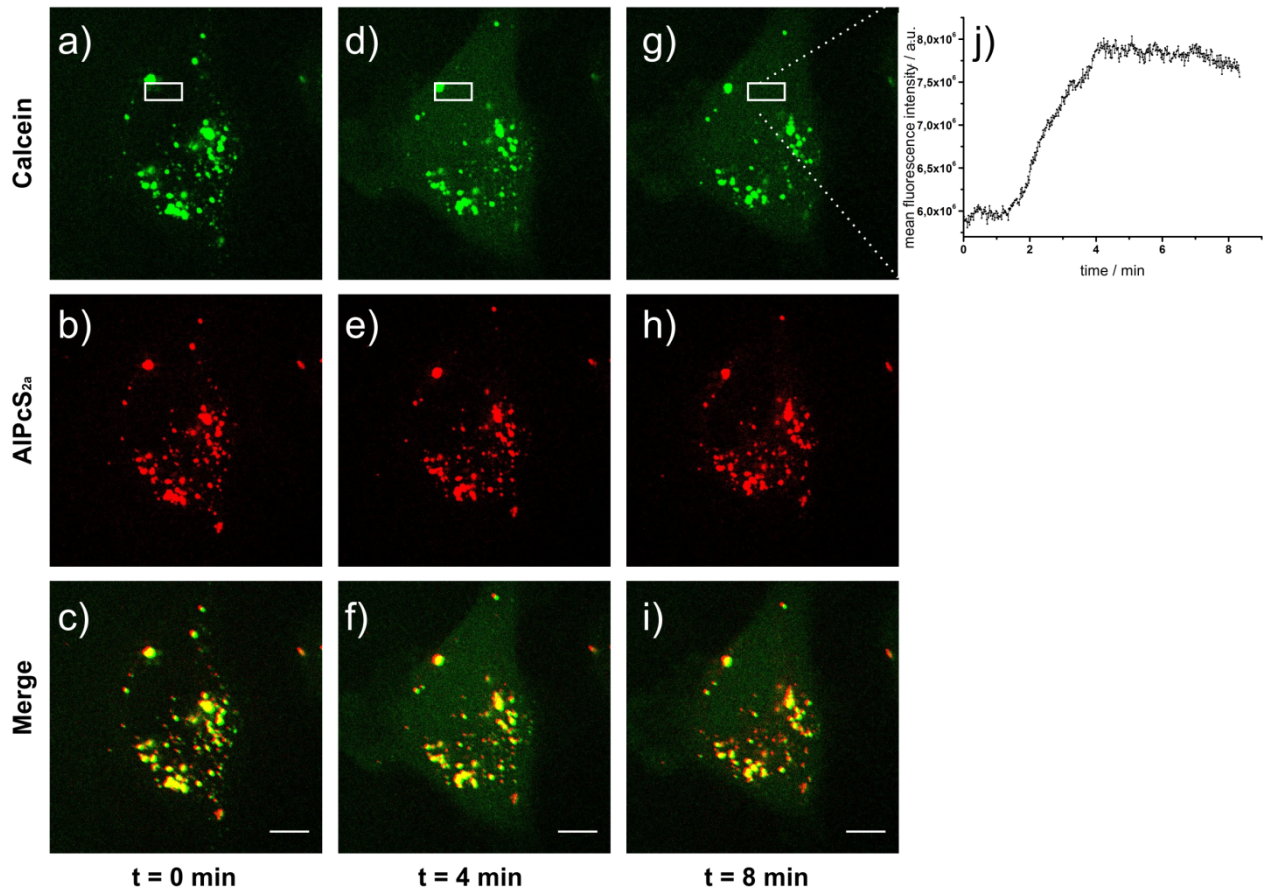


Figure S10. Fluorescence microscopy of MSN-PVP-PEG-AIPcS_{2a}-FA (25 μ g/mL) nanoparticles loaded with calcein inside HeLa cells after 24 h incubation. a-c) Calcein (green) and AIPcS_{2a} (red) are co-localized (yellow) prior to photoactivation. The cell was constantly monitored with a frame rate of 1 frame/s and 0.6 W/mm² of red light (639 nm). d-i) example images after different time points; spreading of calcein can be clearly seen over time, whereas AIPcS_{2a} stays at the same location. j) Intensity of calcein fluorescence inside the cytosol over time in the indicated rectangle, after approximately 2 min an increase can be monitored. The scale bar represents 10 μ m.

In comparison to Figure S10, the incubation of cells with free photosensitizer and free calcein (Figure S11) does not lead to the same effect. It is possible to detect calcein in the beginning of the experiment, but the endocytosed amount is too low to be detected after some time and therefore no spreading could be observed. In contrast to the dot-like pattern of the particle-bound photosensitizer in Figure S10, the spreading of the free photosensitizer can be detected in Figure S11.

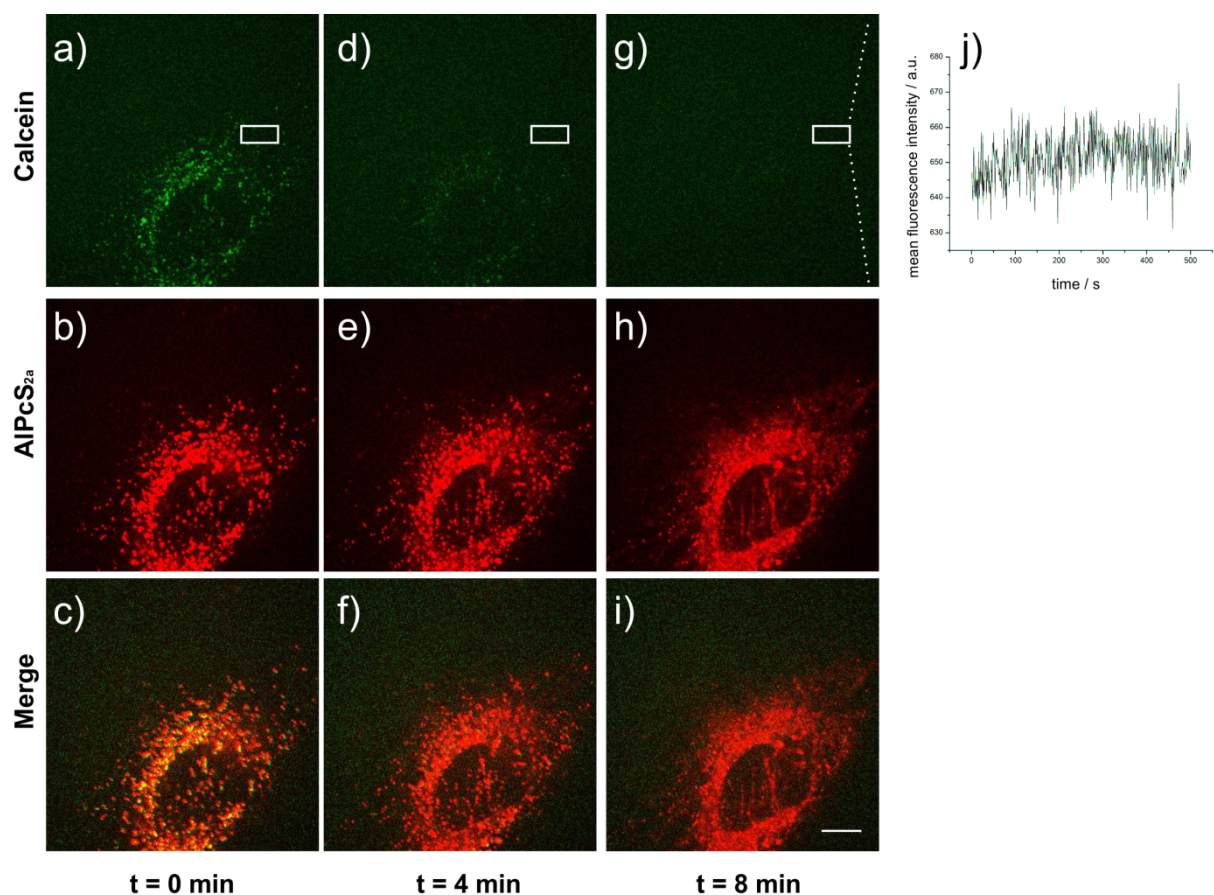


Figure S11. Fluorescence microscopy of free calcein and free AlPcS_{2a} (each 2.5 $\mu\text{g}/\text{mL}$) inside HeLa cells after 24h incubation. a-c) Calcein (green) and AlPcS_{2a} (red) are co-localized (yellow) prior to photoactivation. The cell was constantly monitored with a frame rate of 1frame/s and 0.6 W/mm² of red light (639 nm). d-i) example images after different time points, spreading of AlPcS_{2a} can be clearly seen over time, whereas the calcein fluorescence is too weak to be detected after some time. j) Intensity of calcein fluorescence inside the cytosol over time in the indicated rectangle; no increase inside the cytosol can be detected. The scale bar represents 10 μm .

S7.2. Release of the membrane permeable cargo colchicine

Figure S12 demonstrates the release of colchicine inside cancer cells. As colchicine hinders the polymerization of the tubulin network, cells with GFP labeled tubulins were used. In the case of particle addition, the tubulin structure is completely destroyed and only a uniform fluorescence across the whole cytoplasm could be detected. In the case of untreated cells the tubulin network can be clearly observed.

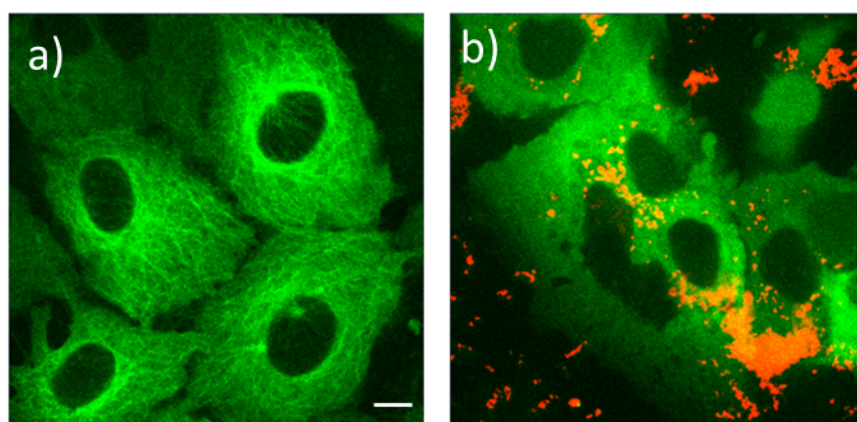


Figure S12. Fluorescence microscopy of HuH7 cell expressing tubulin GFP (green). a) untreated cells. b) MSN-PVP-PEG nanoparticles loaded with colchicine and labeled with Atto 633 (red) after 18 h incubation on the cells. The scale bar represents 10 μm .

S8. Stability tests

S8.1. Nitrogen sorption

After immersion of the particles in DMEM for different times at different pH, they were extensively washed and dried from an acidified (several droplets of 0.01 M HCl) aqueous solution at 60 °C to obtain opened particles for sorption experiments. Nitrogen sorption measurements were performed on a Quantachrome Instruments NOVA 4000e at 77 K. It can be seen that all isotherms maintain the shape of a type IV isotherm. Additionally, no changes in the NLDFT pore size distribution are observed, which shows that the pore structure is not affected by the medium.

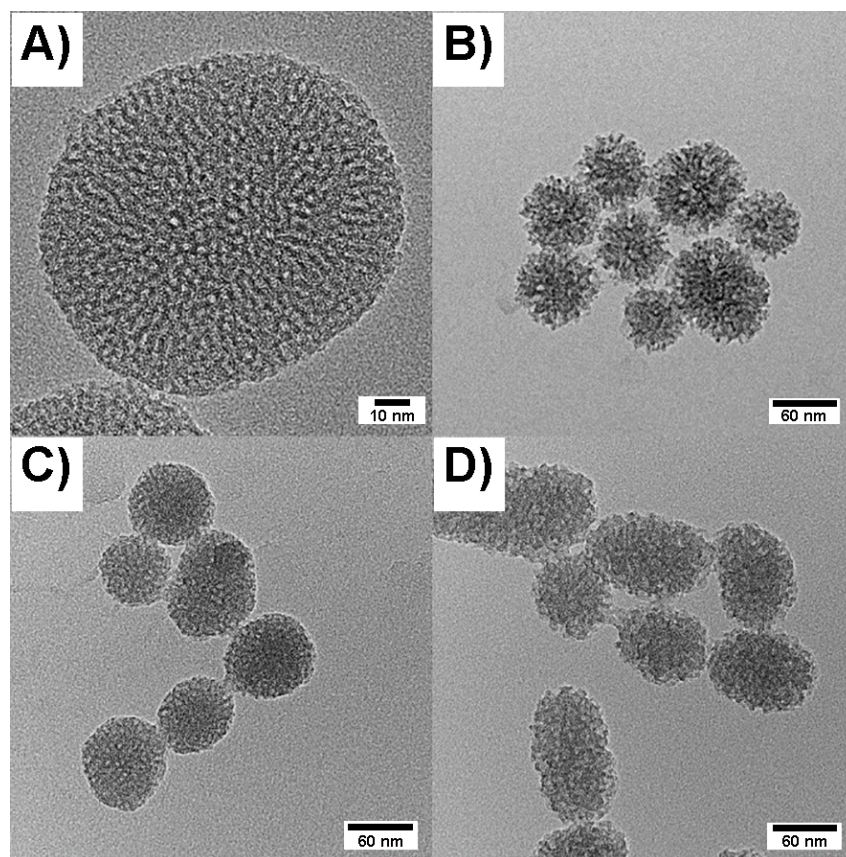


Figure S13. TEM images of A) template-free, untreated MSN-NH₂, B) MSN-NH₂ after 24 h incubation in DMEM, C) MSN-PVP-PEG at pH 7 (closed state) after 24 h in DMEM and D) MSN-PVP-PEG incubated in DMEM at pH 5 (open state) after 24 h.

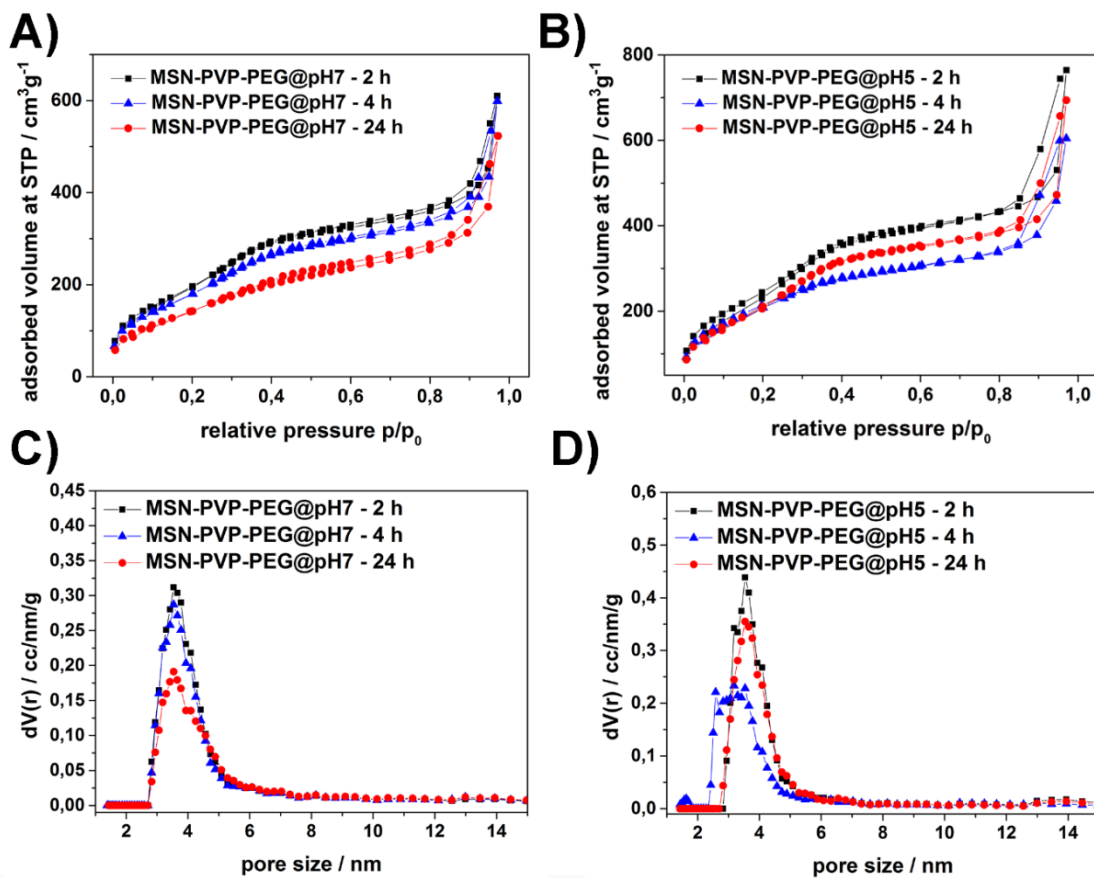


Figure S14: Nitrogen physisorption data of MSN-PVP-PEG after immersion in DMEM at different pH values after 2 h (black), 4 h (blue) and 24 h (red). **A)** Nitrogen sorption isotherms of MSN-PVP-PEG at pH 7, **B)** nitrogen sorption isotherms after immersion in DMEM at pH 5, **C)** pore size distributions of MSNs for different immersion times in DMEM at pH 7 and **D)** at pH 5 after distinct times.

S8.2. Release in cells with three week old particles

Cell experiments also revealed the good stability of the system. Even after storage of the ready-for-use particles for four weeks at 4 °C the release behavior stays the same, as can be seen in Figure S15. This test is in good agreement with the stability tests that are described above. It clearly demonstrates the good shielding of the silica core by the polymer layer.

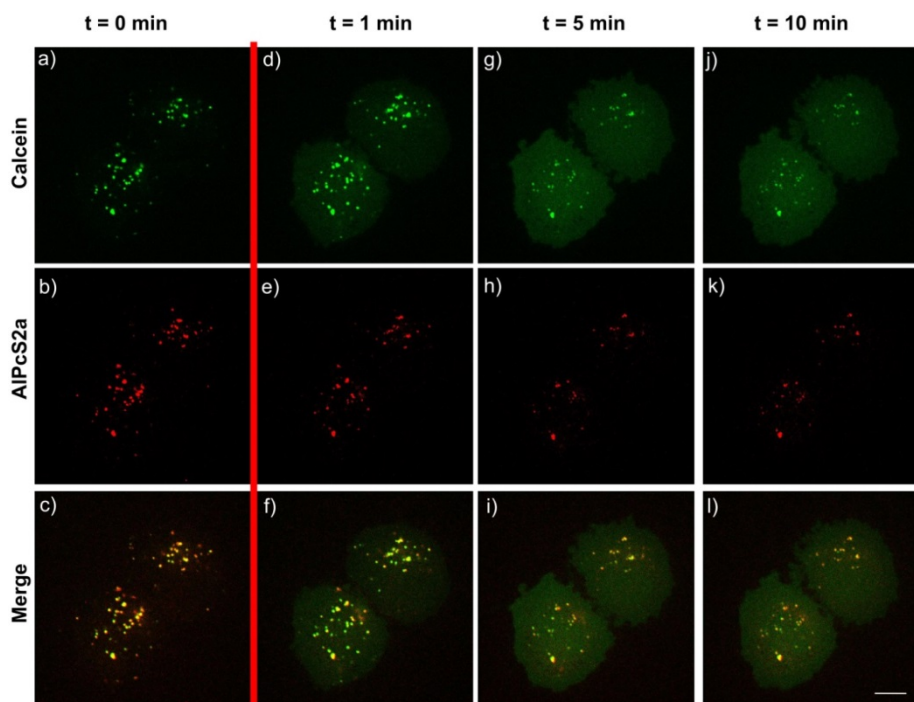


Figure S15. Fluorescence microscopy of MSN-PVP-PEG-AIPcS_{2a}-FA nanoparticles loaded with calcein inside KB cells; particles had been stored three weeks at 4 °C. a-c) Calcein (green) and AIPcS_{2a} (red) are co-localized (yellow) prior to photoactivation. The red line indicates photoactivation with 1.2 W/mm² of red light (639 nm). d-f) after 1 min. photoactivation, h-i) 5 min. after photoactivation, j-l) 10 min. after photoactivation. The scale bar represents 10 μm.

S8.3. DLS measurement for redispersed MSN-PVP-PEG

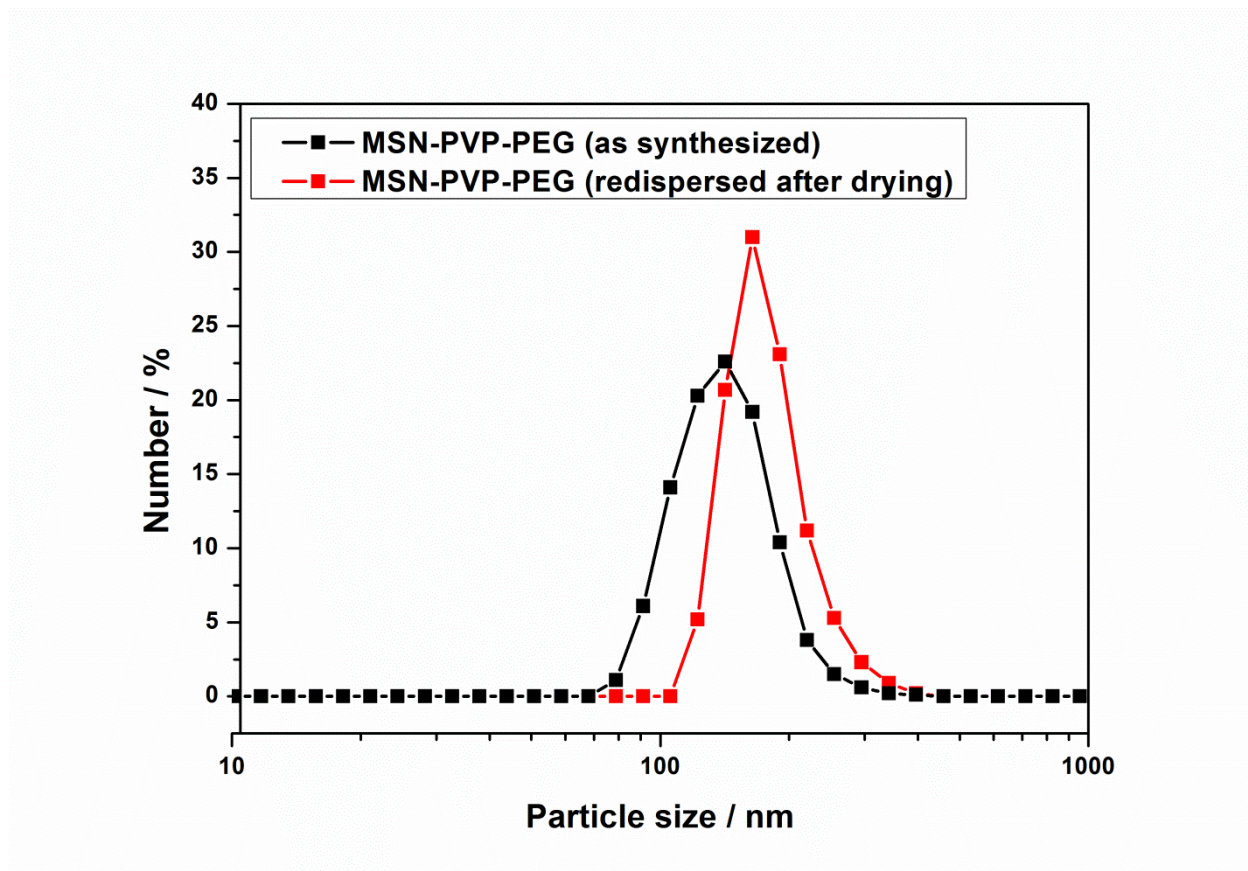


Figure S16. Dynamic light scattering of MSN-PVP-PEG as synthesized (black curve) and after drying the particles, followed by redispersion in water (red curve). There is only a small apparent size increase from around 142 nm to around 164 nm, which demonstrates good redispersability.

S9. In vivo experiments

In Vivo Experiments:

For in vivo experiments female Rj:NMRI-nu (nu/nu) (Janvier, Le Genest-St-Isle, France) mice were housed in isolated ventilated cages with a 12 h day/night cycle and food and water ad libitum. Animal experiments were performed according to guidelines of the German law of protection of animal life and were approved by the local animal experiments ethical committee.

MSN biodistribution: MSN were prepared in HEPES (20mM, Biomol GmbH) with 5% glucose (Merck) (HBG). For analysis of MSN, mice were anesthetized with 3% isoflurane (CP-Pharma) in oxygen. A 100 µg (5 mg/kg) dose of Cy-7 loaded MSN-PVP-PEG-NH₂-FA or unfunctionalized MSN dispersed in 200 µl HBG was injected intravenously into the tail vein of tumor-free mice. Near-infrared fluorescence imaging by a CCD camera using the IVIS Lumina system with Living Image software 3.2 (Caliper Life Sciences, Hopkinton, MA, USA) was started immediately after injection and was repeated after 0.25, 0.5, 1, 4, 24 and 48 h.

Clinical chemistry and histopathology: Mice (n=9) were sacrificed with isoflurane (Isofluran CP®, CP-Pharma) 48 h after intravenous injection of pure HBG or a 100 µg (5 mg/kg) dose of Cy-7 loaded MSN-PVP-PEG-NH₂-FA or unfunctionalized MSN. Blood was collected in serum tubes (Multivette, Sarstedt) and clinical chemistry parameters (alanine transaminase/aspartate transaminase, creatinine levels and blood urea nitrogen) were analyzed. Organs were dissected and fixed in formalin, embedded into paraffin and stained with eosin and hematoxylin. Results were documented using an Olympus BX41 microscope (Olympus, Germany).

S9.1. Biodistribution and biocompatibility upon intravenous injection in mice.

The biodistribution of unfunctionalized MSNs and MSNs functionalized with FA and the cap system was evaluated in vivo. Unfunctionalized and MSN with functionalizations have already been evaluated in literature.^[2] Cy7-loaded MSNs were injected in mice (n=3) via the tail vein. Near infrared fluorescence imaging revealed short circulation times for both particle types (Figure S17).

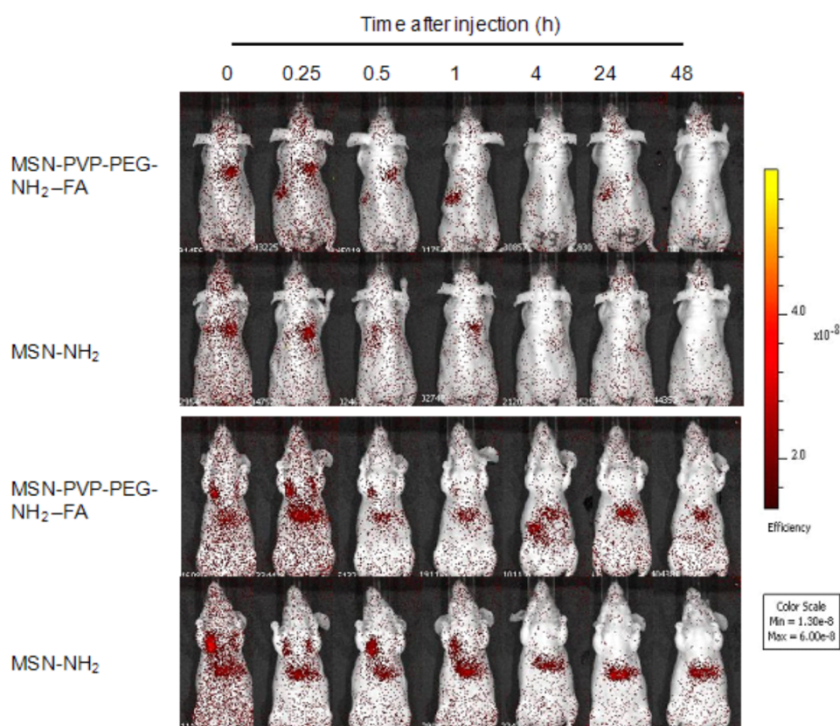


Figure S17: Intravenous administration of MSN in mice examined through near infrared fluorescence imaging. Time-dependent distribution of 100 μg per animal Cy7-loaded MSN-PVP-PEG-NH₂-FA or unfunctionalized MSN (MSN-NH₂) over 48 h. Upper panel: ventral position. Lower panel: dorsal position. Experiments were performed in triplicates; a representative mouse of each group is shown.

Preferred accumulation in the liver was observed for several days (Figure S16). Importantly, both particle types were well tolerated by the mice. To rule out toxic effects of the Cy7-loaded MSN, clinical chemistry parameters were investigated. Serum parameters of 3 mice per group are shown in Table S1. Treatment with functionalized and unfunctionalized particles showed no

deviations from the alanine transaminase (ALT) and aspartate transaminase (AST) levels compared to the control group treated with pure HBG indicating intact liver function. Besides serum, creatinine levels and blood urea nitrogen (BUN) were also unaffected, confirming that kidney function was not compromised by the treatment. Additionally, histopathological examinations of liver, lung, spleen and kidney were carried out, and there were no histological disturbances for both particle types compared to the HBG treated group (Figure S18). A study of He et al. is in good agreement with these results; the authors observed no tissue toxicity for the investigated MSNs and PEGylated MSNs within one month.^[3]

The test of the biocompatibility was carried out with increased dosages in a further experiment. Therefore tumor free NMRI nude mice were injected twice (one week distance) intravenously with a 1.6 mg (80 mg/kg) or 2mg (100 mg/kg) dose of MSN-PVP-PEG-NH₂-FA and MSN-NH₂. There wasn't any visual sign of toxicity at the application of the dosages. Furthermore we observed a slight retention effect after intratumoral application of MSN-PVP-PEG-NH₂-FA into KB tumor bearing mice compared to intratumoral application of MSN-PVP-PEG-NH₂.^[4]

S9.2. Clinical chemistry parameters of the treated animals

Table S1. Clinical chemistry parameters of mice 48 h after treatment with HBG (control), MSN-PVP-PEG-NH₂-FA or unfunctionalized MSN. Values shown: alanine transaminase (ALT); aspartate transaminase (AST); creatinine; blood urea nitrogen (BUN).

Treatment group	ALT (U/I) ±	AST (U/I) ±	Creatinine (mg/dl) ±	BUN (mg/dl) ±
	SD	SD	SD	SD
control	33.9 ± 12.9	54.7 ± 14.1	0.3 ± 0.0	47.3 ± 8.5
MSN-PVP-PEG-NH ₂ -FA	43.2 ± 13.6	59.2 ± 12.1	0.3 ± 0.0	43.9 ± 6.7
MSN-NH ₂	32.5 ± 2.5	51.9 ± 2.1	0.3 ± 0.0	47.4 ± 6.5

S9.3. Histopathological examination of the treated animals

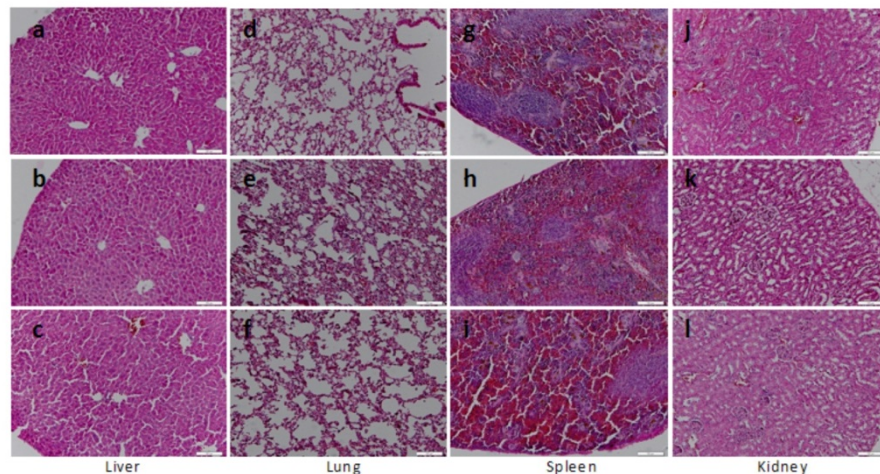


Figure S18. 48 h after treatment with HBG (control), MSN-PVP-PEG-NH₂-FA or unfunctionalized MSN the organs were dissected and fixed in formalin, embedded into paraffin and stained with eosin and hematoxylin. Images were taken on an Olympus BX41 microscope. Histopathological sections of: a) liver of the control (HBG), b) animals treated with functionalized MSN and c) treated with unfunctionalized MSN; d) lung after treatment with HBG, e) functionalized MSN or f) unfunctionalized MSN; g) spleen after treatment with HBG, h) functionalized MSN or i) unfunctionalized MSN; j) kidney after treatment with HBG, k) functionalized MSN or l) unfunctionalized MSN.

- [1] J. Huotari, A. Helenius, *Embo J* **2011**, *30*, 3481-3500.
- [2] a) J. Lu, M. Liong, Z. Li, J. I. Zink, F. Tamanoi, *Small* **2010**, *6*, 1794-1805; b) F. Tang, L. Li, D. Chen, *Advanced Materials* **2012**, *24*, 1504-1534; c) Y. Chen, H. Chen, J. Shi, *Advanced Materials* **2013**, *25*, 3144-3176.
- [3] Q. He, Z. Zhang, F. Gao, Y. Li, J. Shi, *Small* **2011**, *7*, 271-280.
- [4] A. Herrmann, MD thesis 2015: In vivo evaluation of polymeric nanocarriers for targeted gene delivery and novel strategies to overcome chemoresistance. LMU Munich.

List of abbreviations

AlPcS2a	aluminium (III) Pphthalocyanine chloride tetrasulfonic acid
ALT	alanine transaminase
APTES	(3-aminopropyl)triethoxysilane
AST	aspartate transaminase
BET	Brunauer, Emmett und Teller
BUN	blood urea nitrogen
CTAC	cetyltrimethylammonium chloride
DAPI	4,6-diamidino-2- phenylindole dihydrochloride
Dox	doxorubicin hydrochloride
DLS	dynamic light scattering
DMEM	dulbecco's modified eagle's medium
DMSO	dimethyl sulfoxide
dsDNA	double stranded deoxyribonucleic acid
EDC	N-(3-dimethylaminopropyl)-N-ethylcarbodiimide hydrochloride
EPR	enhanced permeability and retention
EtOH	ethanol
FA	folic acid
GFP	green fluorescent protein
HEPES	4-(2-hydroxyethyl)-1-piperazineethanesulfonic acid
HBG	20mM HEPES with 5% glucose
Mn	number average molar mass
MTES	(3-mercaptopropyl)-triethoxysilane
MTT	3-(4,5-dimethylthiazol-2-yl)-2,5-diphenyltetrazolium bromide
MSN	mesoporous silica nanoparticles
NHS	N-hydroxysuccinimid
NLDFT	non-local density functional theory
PDI	polydispersity index
PEG	poly(ethylene glycol)
PEI	polyethylenimine
PNiPAM	poly(N-isopropylacrylamide)
PS	photosensitizer
PVP	poly(2-vinylpyridine)
Rcf	relative centrifugal force
Rpm	revolutions per minute
SSC	saline-sodium citrate buffer
TEA	triethanolamine
TEM	transmission electron microscopy
TEOS	tetraethyl orthosilicate
TFA	trifluoroacetic acid
THF	tetrahydrofuran
WGA	wheat germ agglutinin